In-depth Correlation Power Analysis Attacks on a Hardware Implementation of CRYSTALS-Dilithium

Huaxin Wang[1], Yiwen Gao[1*], Yuejun Liu[1], Qian Zhang[2,3], and Yongbin Zhou[1,2,3]

[1] School of Cyber Science and Engineering, Nanjing University of Science and Technology, China
[2] Institute of Information Engineering, Chinese Academy of Sciences, Beijing, China
[3] School of Cyber Security, University of Chinese Academy of Sciences, Beijing, China
[*]Corresponding author: Yiwen Gao, gaoywin@gmail.com
Email: huaxinwang290@gmail.com, gaoywin@gmail.com, liuyuejun@njust.edu.cn, zhangqian@iie.ac.cn, zhouyongbin@njust.edu.cn

Abstract. During the standardisation process of post-quantum cryptography, NIST encourages research on side-channel analysis for candidate schemes. As the recommended lattice signature scheme, CRYSTALS-Dilithium, when implemented on hardware, has only been subjected to the side-channel attack presented by Steffen et al. in IACR ePrint 2022. This attack is not complete and requires excessive traces. Therefore, we investigate the leakage of an FPGA (Kintex7) implementation of CRYSTALS-Dilithium using the CPA method, where with a minimum of 70000 traces partial private key coefficients can be recovered. As far as we know, this is the first work that applies power leakage to side-channel attacks on FPGA implementations of CRYSTALS-Dilithium. Furthermore, we optimise the attack by extracting Point-of-Interests using known information due to parallelism (named CPA-PoI) and by iteratively utilising parallel leakages (named CPA-ITR). We experimentally demonstrate that when recovering the same number of key coefficients, the CPA-PoI and CPA-ITR reduce the number of traces used by up to 16.67 percent and 25 percent, respectively, compared to the CPA method. When attacking with the same number of traces, the CPA-PoI method and the CPA-ITR method increase the number of recovered key coefficients by up to 55.17 percent and 93.10 percent, respectively, compared to the CPA method. Our experiments confirm that the FPGA implementation of CRYSTALS-Dilithium is also very vulnerable to side-channel analysis.

Keywords: CRYSTALS-Dilithium · Power Analysis Attack · FPGA · Side-Channel Attack · Post-Quantum Cryptography.

1 Introduction

With quantum computers, the conventional public-key cryptographic algorithms, such as RSA, DSA, etc., can be broken by Shor's algorithms [17] without much effort. In response to the threats, National Institute of Standards and Technology (NIST) initiated a post-quantum cryptography (PQC) standardisation process in December 2016 [12], and finally four algorithms were announced for standardisation in July 2022, with CRYSTALS-Kyber [1] being selected as a post-quantum Key Encapsulation Mechanism (KEM), and CRYSTALS-Dilithium (Dilithium for short) [9], Falcon [10], and SPHINCS+ [4] being selected as post-quantum signature schemes. Amongst the signature schemes, NIST primarily recommends Dilithium, as it believes this is the primary algorithm for digital signatures.

Dilithium ensures Strong existential Unforgeability under Chosen Message Attacks (SUF-CMA), and its security is guaranteed by lattice-based hard problems. The security of cryptographic algorithms theoretically lies on their mathematical structures, but in practice, they are also under threat of side-channel attacks (SCAs). The importance of side-channel security for post-quantum cryptography is also emphasised in the NIST PQC standardisation process. Existing side-channel attacks on implementations of Dilithium typically target the random number generation, Number-Theoretic Transform (NTT), or polynomial multiplication operations. Side-channel leakage from these target operations has been investigated using various methods, including Simple Power Analysis (SPA), Correlation Power Analysis (CPA), and profiled attacks. However, current research mostly focuses on software implementations, having little concern on SCA to hardware implementations of Dilithium. In light of this, we study the security of hardware implementations of Dilithium under side channel attacks.

In this paper, we investigate the vulnerable regions of Dilithium and propose practical side-channel attacks to recover the private key by analysing a typical Field-Programmable Gate Array (FPGA) implementation of Dilithium.

1.1 Related Work

Typical implementations of Dilithium is based on ARMs or FPGAs. For ARM-based implementations, Ravi et al. proposed a non-profiled side-channel attack targeting polynomial multiplication, by which partial private key was extracted and utilized to forge signatures [15]. However, they believe that the attack goes beyond polynomial time. Subsequently, Chen et al. proposed a conservative CPA method to reduce the key guessing space and a fast two-stage method to further reduce the guessing space for attacking polynomial multiplication operations [6]. As a result, they were able to fully recover the private key with only 157 power traces. Qiao et al. [14] proposed a new non-profiled attack method, called Public Template Attack (PTA), on both unprotected and protected implementations of Dilithium, targeting the random polynomial $\mathbf{y}$, successfully recovering the private keys. Non-profiled attacks focus primarily on polynomial multiplication, while profiled attacks focus primarily on NTT operations. Primas et al. [13]

proposed a generic method targeting NTT operations that requires establishing templates for all possible multiplications in butterfly operations, which is costly. Han et al. [11] employed a machine learning-based method to attack NTT operations, recovering keys using 60000 power traces. Berzati et al. [5] reconstructed a given coefficient in a predicted vector to determine if it is zero, thus recovering the private key using linear algebra methods, with 700000 power traces.

In FPGA-based implementations, Steffen et al. [18] proposed the first side-channel attack targeting polynomial multiplication in Dilithium using electromagnetic analysis. They analyzed two polynomial multiplication operations: $c\mathbf{t}_0$ and $c\mathbf{s}_1$ (where $c\mathbf{t}_0$ does not affect the security of the Dilithium scheme). However, in their analysis of $c\mathbf{s}_1$, they only provided results for one key coefficient, and under 1000000 electromagnetic traces, the Pearson correlation coefficient for the correct key was not significant. Additionally, they also performed profiled analysis on NTT operations and successfully recovered the private key using 700000 electromagnetic traces. However, the capabilities of the adversary set in their experiment were excessively strong.

Among the mentioned works, only Steffen et al. [18] conducted attacks on an FPGA-based implementation of Dilithium, but they did not analyse more key coefficients. Moreover, due to the high cost of establishing templates in profiled attacks, this paper only focuses on non-profiled attacks.

1.2 Contributions

The contributions of this paper are summerised as follows:

- An analysis of the characteristics of Dilithium hardware implementation has been conducted, showing the CPA side-channel attacks on polynomial multiplication, providing the first results of using power leakages for side-channel analysis on it. In this analysis, it has been demonstrated that it is possible to recover partial keys with a minimum usage of 70000 power traces.
- By extracting Point-of-Interests (PoIs) from known information about the algorithm execution, we propose the CPA-PoI method. Compared to the CPA attack, it reduces the algorithm's complexity and also decreases the number of power traces required for the attack, with a reduction of up to 16.67%. Its average Guessing Entropy is lower than that of the CPA method. When attacking with the same number of power traces, the number of recovered key coefficients is increased by up to 55.17%.
- Taking advantage of the highly parallelized implementation in FPGA, we propose a better characterization of leakage features with the CPA-ITR method. Compared to the CPA method, this method reduces the number of power traces used by up to 25%. At the same time, when attacking with the same number of power traces, the number of recovered key coefficients can be improved by up to 93.10%.

1.3 Organisations

The structure of this paper is as follows: **Section** 2 provides notations involved in this paper, and gives a brief introduction to Dilithium v3.1 signature scheme. It also introduces the target FPGA implementation and Correlation Power Analysis. **Section** 3 provides a detailed description of target operation and methods proposed in this paper. **Section** 4 introduces the experimental setups and analyses the experimental results of our attacks. Finally, conclusions are given in **Section** 5.

2 Preliminaries

2.1 Notations

Let n and q be two integers, where $n = 256$ and $q = 8380417 = 2^{23} - 2^{13} + 1$. We use R_q to denote the polynomial ring $\mathbb{Z}[x]/(x^n + 1)$, the infinity norm $||x||_\infty$ denotes the maximum absolute value among all coefficients of a polynomial x. For a polynomial vector, this norm is defined as the maximum infinity norm of all polynomials in the vector. Therefore, S_b denotes the set of polynomials in R_q with infinity norm equal to b, while $\tilde{S}_b$ denotes the same set but excluding coefficients with value $-b$. Additionally, the set of polynomials in R_q with exactly τ nonzero coefficients and infinity norm equal to 1 is denoted as B_τ. We use bold lowercase letters to denote vectors (e.g. $\mathbf{v}$), and bold uppercase letters to denote matrices (e.g. $\mathbf{A}$). Polynomials in the NTT domain are denoted with a hat (e.g. $\hat{c}$, $\hat{c} = \mathrm{NTT}(c)$). This notation is transitive, so $\hat{\mathbf{s}}$ denotes each polynomial in $\mathbf{s}$ being individually transformed into the NTT domain. Finally, we use $\circ$ to denote pointwise multiplication. $\mathrm{HD}(a \circ b)[i]$ denotes the value of the Hamming distance after calculating the i-th coefficient of the register storing the computation result of $a \circ b$.

2.2 CRYSTALS-Dilithium

Dilithium consists of three algorithms: key generation, signature generation, and signature verification. Because the signature verification is unrelated to the attacks mentioned in this paper, it will not be further introduced here.

Key Generation The key generation process generates a private key for signature generation and a public key for verification, as shown in **Algo**. 1. From this, it can be seen that finding the private key from the public key is essentially equivalent to solving the M-LWE problem. Additionally, once an attacker obtains either value $\mathbf{s}_1$ or $\mathbf{s}_2$, they can derive the other value directly since $\mathbf{A}$ and $\mathbf{t}$ are public values. The Power2Round function is used to split the M-LWE problem instance $\mathbf{t}$ into high and low bits in order to compress the size of the public key.

Algorithm 1 Key Generation

```
1: $\zeta \leftarrow \{0,1\}^{256}$
2: $(\rho, \rho', K) \in \{0,1\}^{256} \times \{0,1\}^{512} \times \{0,1\}^{256}$ :=H($\zeta$)
3: $\mathbf{A} \in R_q^{k \times \ell}$ :=ExpandA($\rho$)
4: $(\mathbf{s}_1, \mathbf{s}_2) \in S_\eta^\ell \times S_\eta^k$ := ExpandS($\rho'$)
5: $\mathbf{t} := \mathbf{A}\mathbf{s}_1 + \mathbf{s}_2$
6: $(\mathbf{t}_1, \mathbf{t}_0) :=$ Power2Round$_q(\mathbf{t}, d)$
7: $tr \in \{0,1\}^{256} :=$ H($\rho||\mathbf{t}_1$)
8: return (pk = $(\rho, \mathbf{t}_1)$, sk = $(\rho, K, tr, \mathbf{s}_1, \mathbf{s}_2, \mathbf{t}_0)$)
```

Signature Generation The signature generation process is shown in **Algo**. 2. It begins by recomputing **A** and hashing the message M along with the hash value of the public key tr. The loop is terminated by generating noise $\mathbf{y} \in S^\ell_{(\gamma_1-1)}$ using the ExpandMask function. Compress the $\mathbf{w} = \mathbf{Ay}$ to $\mathbf{w}_1$ using the HighBits function. The hint $\mathbf{h}$ allows the verifier to recompute $\mathbf{w}_1$. The hash function H instantiates the random oracle required in the proof. It returns a sparse ternary polynomial $c \in B_{60}$, which has a Hamming weight of 60 and all non-zero coefficients equal to $+1$ or -1. The Decompose function returns both HighBits and LowBits of its input. Finally, the check is performed to determine if the current signature is rejected, and if so, it is recomputed. Otherwise, the signature $\sigma = (\tilde{c}, \mathbf{z}, \mathbf{h})$ is generated.

Dilithium Parameters The first submission [8] to the PQC competition underwent several parameter modifications during the NIST PQC standardisation process. The current version can be found in [2], and compared to the previous submission [7], the main adjustments were made to the k and ℓ dimensional parameters in order to better comply with NIST's security levels. The parameters of the current version 3.1 can be seen in the **Table** 1.

Table 1: Dilithium Parameters for version 3.1 (Dilithium v3.1)

Parameter Set	Value		
Security Level	2	3	5
τ [# of $\pm$1's in c]	39	49	60
ω [max # of 1's in hint $\mathbf{h}$]	80	55	74
(k, ℓ) [Dimensions of $\mathbf{A}$]	(4,4)	(6,5)	(8,7)
η [secret key range]	2	4	2
q [Modulus]	8380417		
d [dropped bits from $\mathbf{t}$]	13		

Algorithm 2 Signature Generation

```
1: $\mathbf{A} \in R_q^{k \times \ell} := \mathrm{ExpandA}(\rho)$
2: $\mu \in \{0,1\}^{512} := \mathrm{H}(tr||M)$
3: $\kappa := 0$, $(\mathbf{z}, \mathbf{h}) := \perp$
4: $\rho' \in \{0,1\}^{512} := \mathrm{H}(K||\mu)$
5: while $(\mathbf{z}, \mathbf{h}) = \perp$ do
6:     $\mathbf{y} \in \tilde{S}_{\gamma_1}^{\ell} := \mathrm{ExpandMask}(\rho', \kappa)$
7:     $\mathbf{w} := \mathbf{Ay}$
8:     $\mathbf{w}_1 := \mathrm{HighBits}_q(\mathbf{w}, 2\gamma_2)$
9:     $\tilde{c} \in \{0,1\}^{256} := \mathrm{H}(\mu||\mathbf{w}_1)$
10:    $c \in B_\tau := \mathrm{SampleInBall}(\tilde{c})$
11:    $\mathbf{z} := \mathbf{y} + c\mathbf{s}_1$
12:    $\mathbf{r}_0 := \mathrm{LowBits}_q(\mathbf{w} - c\mathbf{s}_2, 2\gamma_2)$
13:    if $\|\mathbf{z}\|_\infty \geq \gamma_1 - \beta$ or $\|\mathbf{r}_0\|_\infty \geq \gamma_2 - \beta$ then
14:        $(\mathbf{z}, \mathbf{h}) := \perp$
15:    else
16:        $\mathbf{h} := \mathrm{MakeHint}_q(-c\mathbf{t}_0, \mathbf{w} - c\mathbf{s}_2 + c\mathbf{t}_0, 2\gamma_2)$
17:        if $\|c\mathbf{t}_0\|_\infty \geq \gamma_2$ or $\sum h_i > \omega$ then
18:            $(\mathbf{z}, \mathbf{h}) := \perp$
19:        end if
20:    end if
21:    $\kappa := \kappa + \ell$
22: end while
23: return $\sigma = (\tilde{c}, \mathbf{z}, \mathbf{h})$
```

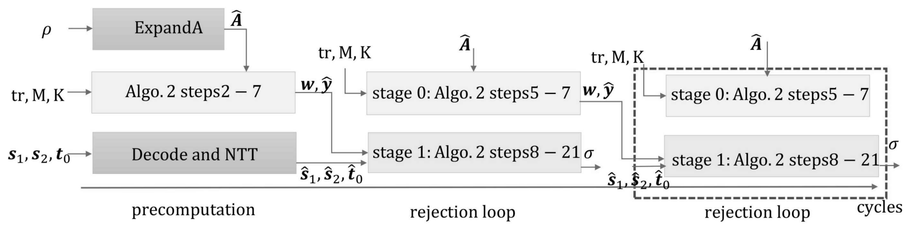

Fig. 1: The architecture of the target FPGA implementation of Dilithium.

2.3 Target FPGA Implementation of Dilithium

Our attacks are conducted on the hardware implementation Dilithium by Bechwith et al. [3]. It is known for its good performance as an FPGA implementation with high speed. The algorithm of the signature generation is shown in **Fig**. 1, which is divided into *pre-computation phase* and *rejection loop phase.* During the pre-computation phase, the key is decoded and transformed into the NTT domain. At the same time, the calculations for $\mathbf{w}$ and $\mathbf{y}$, which are required in the rejection loop (Line 5 to 22 in **Algo**. 2), are computed in advance, and the calculation results are directly provided to generate the signature in the rejection loop. The calculation in the rejection loop is divided into two-stage pipelines, *Stage*-0 and *Stage*-1. Stage-0 prepares for the next Stage-1 calculation. If the generated signature σ passes in Stage-1, it is output as the signature without performing the calculations within the red dashed line. If it fails, the loop continues until a valid signature is generated.

In the implementation, polynomial multiplication (including NTT), addition, and multiplication are implemented through polynomial arithmetic units. It utilizes four butterfly units to process four coefficients in parallel for all operations. For the multiplication, reduction of the computed result is required. The hardware implementation uses Barrett reduction, which can be implemented using only shifting and addition operations.

Therefore, when analysing the implementation of polynomial multiplication, the rejection loop and the polynomial arithmetic units bears a high degree of parallelism, resulting in a large amount of algorithmic noise during side-channel analysis, which affects the attacking results.

2.4 Correlation Power Analysis

Side-channel analysis utilizes the power consumption or electromagnetic information generated by the execution of a cryptographic algorithm on a device in order to extract sensitive information. Correlation Power Analysis (CPA) is one of the methods used in side-channel analysis. It is essentially an improvement of DPA. In practical attacks, the classical CPA typically involves five steps:

- Select an appropriate intermediate value as the attack position. The calculation function of this intermediate value takes the key (or a fixed value from which the key can be derived) and known variables as inputs.
- Collect the power traces of the targeted operation. Execute the signing process n times and store the power traces of each collection, with each trace consisting of m data points, in the matrix $T_{n\times m}$.
- Compute the intermediate value matrix $V_{n\times k}$ for the guessed key. Based on the range of key coefficient values, the size of key guessing space k can be determined. Using the assumed key and known variables, the intermediate values of the targeted operation can be calculated.
- Using an appropriate power consumption model, map the values of the intermediate value matrix $V_{n\times k}$ to the assumed power consumption matrix $H_{n\times k}$ one-to-one.

– Compute the correlation coefficients between the assumed power consumption matrix $H_{n\times k}$ and the actual power consumption matrix $T_{n\times m}$ for each column, and record them in the correlation matrix $R_{k\times m}$. The calculation of correlation coefficients can be done using Pearson's correlation coefficient formula, as shown in **Eq**. 1.

$$R_{i,j} = \frac{\sum_{x=1}^{n}(H_{x,i} - \overline{H}_i)\cdot(T_{x,j} - \overline{T}_j)}{\sqrt{\sum_{x=1}^{n}(H_{x,i} - \overline{H}_i)^2 \cdot \sum_{x=1}^{n}(T_{x,j} - \overline{T}_j)^2}} \tag{1}$$

The index of the maximum value in matrix R corresponds to the leakage point and the key used in the targeted operation.

3 The Proposed Side Channel Attacks

3.1 Vulnerable Region

In the process of Dilithium signature generation, polynomial multiplications are calculated many times. The calculations of $c\mathbf{s}_1$ and $c\mathbf{s}_2$ involve the public variable c, while $\mathbf{s}_1$ and $\mathbf{s}_2$ are both parts of the private key, making them suitable for CPA. This paper focuses on attacking the hardware implementation of $c\mathbf{s}_1$. In the context of Dilithium, c is a polynomial with $n = 256$ coefficients, each ranging from -1 to 1. $\mathbf{s}_1$ is a polynomial vector consisting of ℓ polynomials, with a total of $\ell \times n$ coefficients, each ranging from $-\eta$ to η. To speed up the computation of polynomial multiplication, Dilithium algorithm introduces NTT. Therefore, before performing polynomial multiplication, the polynomials are mapped to the NTT domain and then multiplied using point-wise multiplication, as shown in **Eq**. 2.

$$c\mathbf{s}_1 = \mathrm{INTT}\left(\mathrm{NTT}\left(c\right) \circ \mathrm{NTT}\left(\mathbf{s}_1\right)\right) \tag{2}$$

In the FPGA implementation [3], the polynomial arithmetic unit is responsible for polynomial multiplication (including NTT), addition, and subtraction. The design utilises a 2×2 butterfly structure, which is applied to all polynomial arithmetic operations, enabling parallel processing of four coefficients. Barrett reduction is used for multiplication, which involves fewer multiplications than that of Montgomery reduction.

To avoid leaking the private key, Dilithium employs rejection sampling (Step 5 to 22 in **Algo**. 2), with the loop repetitions of 4.25. The parallelised pipeline design accelerates signature generation. However, it also introduces additional noise during side-channel analysis due to the simultaneously executed operations such as $\mathbf{y} = \mathrm{ExpandMask}(\rho', \kappa)$, which involves the keccak function, in the calculation of $(\hat{c} \circ \hat{\mathbf{s}}_1)$. As shown in **Fig**. 2, different colors are used in the figure to indicate the different states during the execution of keccak. This noise can affect the effectiveness and efficiency of the attack.

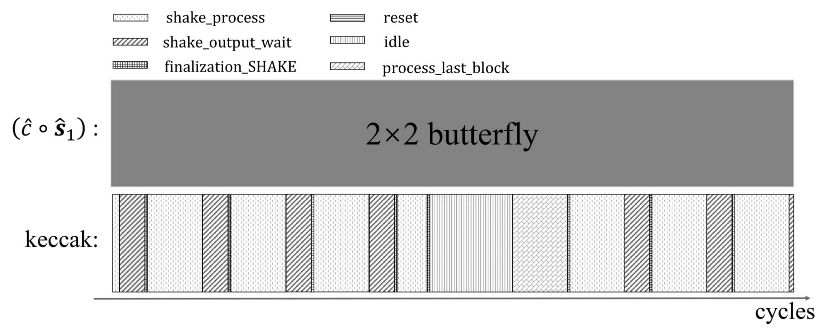

Fig. 2: The overlapping of keccak and $(\hat{c} \circ \hat{\mathbf{s}}_1)$ in the time domain.

3.2 CPA on Polynomial Multiplication

In the C reference implementation of Dilithium, the NTT operation omits the reduction operation to reduce the computational load. After 8 levels of recursive butterfly calculations, a 256-dimensional polynomial yields coefficients in the NTT domain ranging from $[-\eta - 8(q-1), \eta + 8(q-1)]$. At security level 2, where $\eta = 2$ and $q = 2^{23} - 2^{13} + 1$, the size of key guessing space in a CPA is close to 2^{27}. This leads to a relatively large computational complexity when performing CPA on the Dilithium implementation..

However, in the target implementation, Barrett reduction is applied after the butterfly multiplication, which limits the range of polynomial coefficients in the NTT domain to $[0, q)$. Therefore, in the attack on Dilithium, the key guessing space used by the attacker is $[0, q)$.

For software implementations, it is difficult to analyse the continuous numerical processing on the bus, so the Hamming weight of the targeted variable is often used as a leakage model [6], [14]. For hardware implementations, it is possible to analyse the previous reference value of the operation by examining registers, hence the Hamming distance model is commonly used to model the power consumption generated by the targeted operation [18]. The actual power consumption L can be expressed as the Hamming distance between the values before and after (Note: the coefficient index is i) the register is assigned a value, as shown in **Eq**. 3.

$$L = \alpha \times \mathrm{HD}\left(\hat{c} \circ \hat{\mathbf{s}}_1\right)[i] + N \tag{3}$$

where α denotes the scaling factor, and N refers to the noise.

From **Section** 2.4, we learn that the number of points in an power trace directly affects the complexity of calculating the correlation coefficient matrix. In hardware implementation, the value of a register can only change once per clock cycle. Therefore, assuming no clock delay, the variations in register values are closely related to the intervals between points on the power trace in consecutive clock cycles. Specifically, the number of sample points within one clock cycle can be calculated by dividing the sampling rate by the clock frequency. During an attack, the power trace can be sliced to obtain leakage points more accurately. This can be done by adding the current sample point index to the product of the number of sample points and the clock interval for register value changes, in order to determine the location of the leakage point. These leakage points can then be used to replace the entire segment of the power trace, to construct the correlation coefficient matrix.

It should be noted that the above description is based on ideal conditions. However, in practical applications, there is often some delay in the data. Therefore, the selected leakage points during the attack process will be adjusted by plus or minus 15 from their original positions to ensure that the leakage points fall within the selected sample points for the attack.

3.3 CPA-PoI on Polynomial Multiplication

In the attack on $c\mathbf{s}_1$ by Steffen et al. [18], a million electromagnetic traces were utilised. Even when using a million power traces for the attack, the computation scale of the Pearson correlation is still enormous, even with the aforementioned CPA method. In CPA, if PoIs can be accurately selected, it not only reduces the computational scale of the correlation coefficient matrix but also enables a more direct determination of the location of information leakage. Therefore, we first select points by locating the leakage point, and then proceed with the CPA method for the attack, we refer to this attack method as CPA-with-PoI (abbr. **CPA-PoI**).

In side-channel analysis, any points in the power trace that exhibit significant differences are considered as PoIs. In profiled attacks, the selection of the number of PoIs directly affects the size of the Pearson correlation. Therefore, it is necessary to identify the PoIs in order to reduce the size of the templates. Similarly, in CPA, if the PoIs can be accurately selected, it not only reduces the computational complexity of the correlation coefficient matrix but also allows for more direct localization of the leakage position, minimizing the impact of noise.

In the same clock cycle, the timing of value changes for different registers may overlap. This overlap can result in partial repetition or overlap of PoIs in the power traces. Therefore, PoIs of the target operation may coincide with PoIs of other operations. By observing the implemented architecture, it is found that during the computation of $(\hat{c} \circ \hat{\mathbf{s}}_1)[i]$, the $\hat{c}$ needed for subsequent calculations is fetched in advance, thereby generating power consumption. Additionally, due to the 2×2 butterfly structure, there are four consecutive indices of $\hat{c}$ coefficients that can be processed in parallel. The figures obtained by calculating the Pearson correlation using $\hat{c}$, $(\hat{c}\circ\hat{\mathbf{s}}_1)[i]$, and the power traces are shown in **Fig**. 3. It can be seen that the challenge $\hat{c}$ coincides with the PoIs of the key in the power trace, and the correlations with $\hat{c}$ are high. Since $\hat{c}$ is known, it can be used to extract PoIs.

Based on this idea, after using the power trace segmentation method in the aforementioned CPA, the segmented power traces can be further correlated with the known $\hat{c}$ to extract PoIs more accurately.

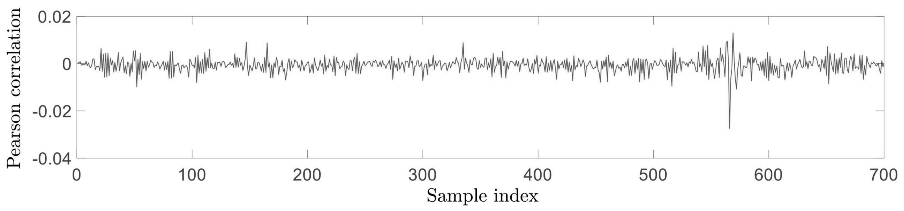

(a) The Pearson correlation between the HDs of $\hat{c}$ and the traces.

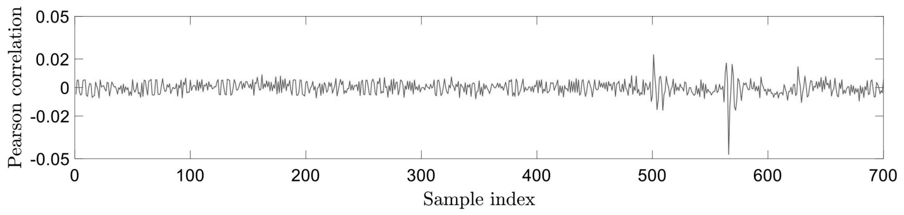

(b) The Pearson correlation between the HDs of $(\hat{c} \circ \hat{\mathbf{s}}_1)[i]$ and the traces.

Fig. 3: The Pearson correlation between the hypothetical leakages related to $c\mathbf{s}_1$ and the traces.

3.4 CPA-ITR on Polynomial Multiplication

In CPA, the Hamming distance of a coefficient's target operation is used as an assumed power consumption. In the FPGA implementation of Dilithium, polynomial multiplication involves the simultaneous use of 2×2 butterfly structures, as shown in **Fig**. 4. The values within the square brackets in the figure denote the coefficient indices of $\hat{c}$ and $\hat{\mathbf{s}}_1$. A good power consumption model can help an attacker accurately identify, extract, or infer sensitive information from the target device. According to **Eq**. 3, for the actual power consumption L generated by the same power trace, the smaller the noise N, the closer the assumed power consumption $(\hat{c} \circ \hat{\mathbf{s}}_1)\,[i]$ is to H. In this case, the attack achieves the best results. A single coefficient's assumed power consumption may not be sufficiently close to the actual power consumption.

At the same moment, the coefficients being processed have indices i, $i+1$, $i+2$ and $i+3$, if only the operation with the coefficient index i is attacked, the other coefficients are considered as part of the noise N, resulting in higher noise levels. Meanwhile, in the scenario of parallel attack on all four coefficients, the size of key guessing space has changed from q to q^4, making the attack more difficult.

In practical attacks, for parallel computations occurring at the same moment, they are usually attacked in the order of their indices. This means that when attacking the operation with index $i+1$, the related value for the operation with index i is already known. Therefore, after recovering the key coefficient with index i using the CPA method (using **Eq**. 4 as the assumed power consump-

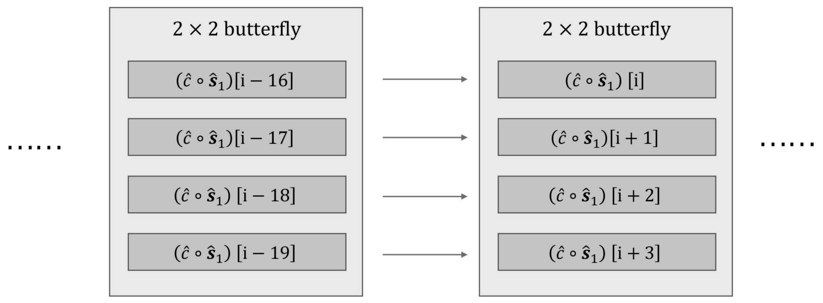
2 × 2 butterfly
$(\hat{c} \circ \hat{\mathbf{s}}_1)[i-16]$
$(\hat{c} \circ \hat{\mathbf{s}}_1)[i-17]$
$(\hat{c} \circ \hat{\mathbf{s}}_1)[i-18]$
$(\hat{c} \circ \hat{\mathbf{s}}_1)[i-19]$
2 × 2 butterfly
$(\hat{c} \circ \hat{\mathbf{s}}_1)[i]$
$(\hat{c} \circ \hat{\mathbf{s}}_1)[i+1]$
$(\hat{c} \circ \hat{\mathbf{s}}_1)[i+2]$
$(\hat{c} \circ \hat{\mathbf{s}}_1)[i+3]$
......
......

Fig. 4: The value of the 2×2 butterfly operation's registers at adjacent cycles.

tion), **Eq**. 5 can be used as the assumed power consumption to recover the key coefficient with index $i+1$, considering that **Eq**. 4 is known. This process can be repeated sequentially, modifying the assumed power consumption model (**Eq**. 6, **Eq**. 7), to better model the leakage and reduce the noise levels.

$$w_1 = \alpha \times \mathrm{HD}\left(\hat{c} \circ \hat{\mathbf{s}}_1\right)[i] \tag{4}$$

$$w_2 = w_1 + \alpha \times \mathrm{HD}\left(\hat{c} \circ \hat{\mathbf{s}}_1\right)[i+1] \tag{5}$$

$$w_3 = w_2 + \alpha \times \mathrm{HD}\left(\hat{c} \circ \hat{\mathbf{s}}_1\right)[i+2] \tag{6}$$

$$w_4 = w_3 + \alpha \times \mathrm{HD}\left(\hat{c} \circ \hat{\mathbf{s}}_1\right)[i+3] \tag{7}$$

where α denotes scaling factors.

Here, due to the parallel nature of the target operation, we store the information obtained from previous attacks and combine it with the assumed power consumption model for subsequent attacks, in order to reduce noise. We refer to the method of dynamically overlaying the assumed power consumption model in CPA attacks as CPA-with-Iteration (abbr. **CPA-ITR**).

4 Experimental Results

Setup The power traces of polynomial multiplication execution in Dilithium are collected on the SAKURA-X development board for side-channel evaluation. The setup is shown in **Fig**. 5, which consists of a *ROHDE* & *SCHWARZ* PA303 30dB pre-amplifier, *PicoScope* 3206D oscilloscope, and SAKURA-X FPGA development board with *Xilinx* Kintex7 XC7K160T chip. The chip runs at 4MHz. The oscilloscope can simultaneously use two channels to sample with a $4ns$ interval (i.e. sampling rate 250MS/s). One channel is used for collecting traces of instant power consumption, and the other is used to trigger for sampling.

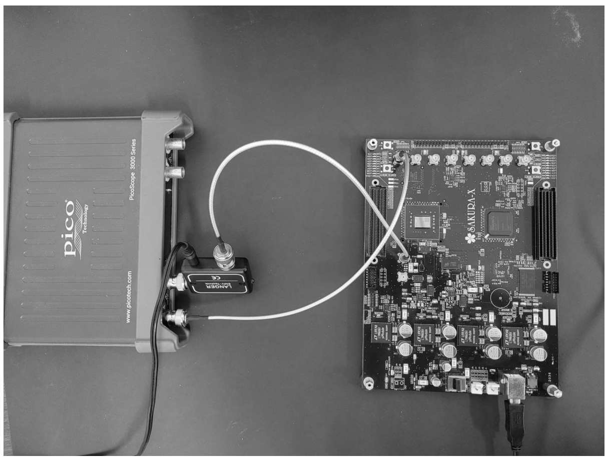

Fig. 5: The setup of our experiments.

Target FPGA Implementation Our target implementation is the FPGA implementation of Dilithium v3.1 in [3]. For the purpose of analysis, the security level is set to 2 (increasing the security level will increase the number of key coefficients but will not make the attack more difficult). It is implemented using both Verilog and VHDL languages. This introduces an delay-optimised FPGA design and covers the three security levels of Dilithium. We programme the signature generation of Dilithium into the SAKURA-X target board and send the message and its length from the PC to the target board for signing. We use the ISE-14.7 Design Suite to programme the Kintex7 XC7K160T chip.

Some Settings The power traces collected for the polynomial multiplication on $c\mathbf{s}_1$ are shown in **Fig**. 6, where a clear periodicity can be observed. Using these traces, an attacker can analyse the key coefficients sequentially. Due to the parallel execution of the keccak function during the polynomial multiplication process, as shown in **Fig**. 2, each state generates different algorithmic noise, which affects the attacks differently. In order to evaluate and compare the results of the attack experiments, we obtained the state of the keccak function execution for each clock cycle through timing simulation and conducted separate attack experiments accordingly. **Fig**. 7 shows the correlation trend of the most likely key guesses for 16761 (i.e. $\lceil \frac{8380417}{500} \rceil$) under the six states of the keccak function, based on different numbers of traces. The correct key guess is indicated in red, where the correct key guesses are marked in red and standing out with more traces. From the graph, it can be observed that a significant correlation is only observed after 700000 power traces for the shake_process and process_last_block states, which leads to a longer attack time. Therefore, in the experimental process of this paper, not all key coefficients were targeted for attack, but only a selected few were chosen based on the target operations present in each state of keccak. For reset and finalization_SHAKE states, there are a total of 8 and 24

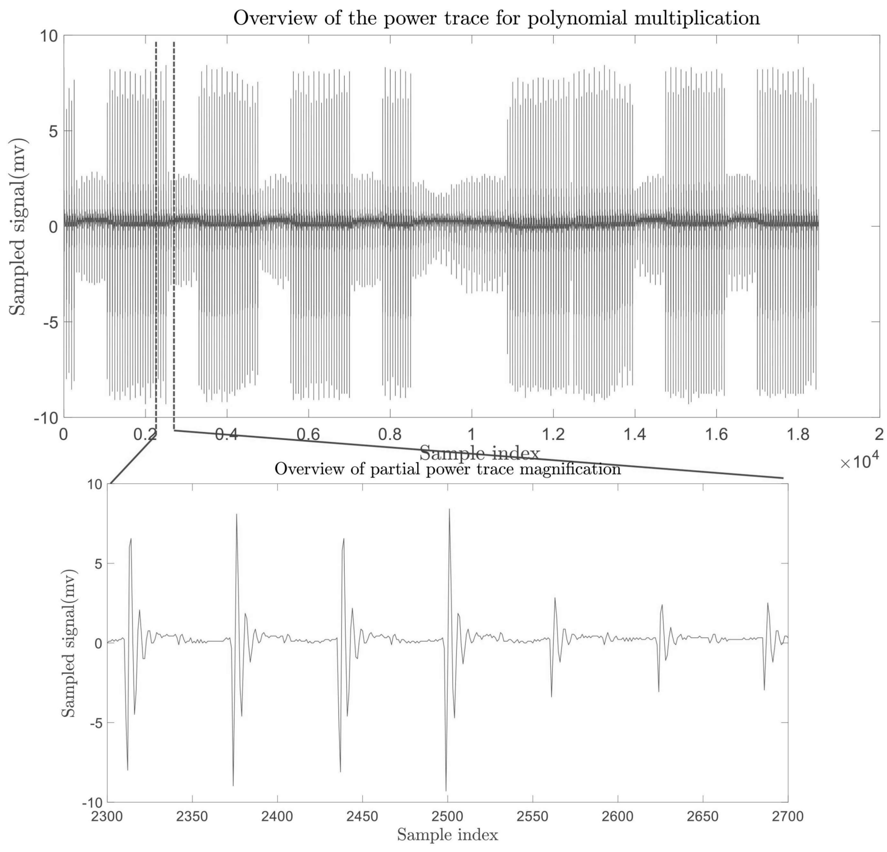

Fig. 6: Power traces of FPGA implementation of Dilithium in our setting.

parallel target operations respectively, so all coefficients were chosen for attack. For shake_output_wait and idle states, which have a larger number of parallel target operations, 64 were selected as reference. Due to the excessively long attack time, only 32 were chosen as reference for the shake_process and process_last_block states.

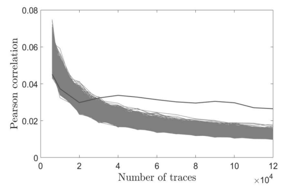

(a) reset

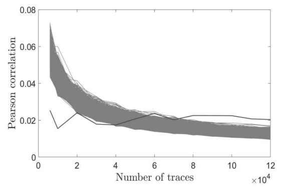

(b) idle

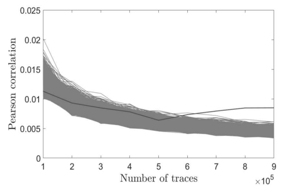

(c) process_last_block

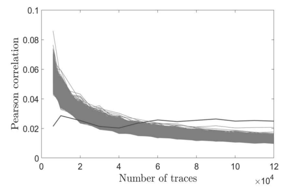

(d) finalization_SHAKE

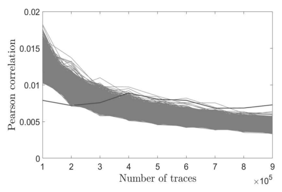

(e) shake_process

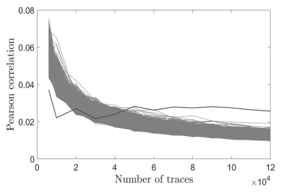

(f) shake_output_wait

Fig. 7: Absolute correlation values for 16761 most likely key guesses with different numbers of traces.

4.1 Results of the CPA Method

First, the CPA method is executed, using the power trace segmentation method for the attack. The calculation complexity at this stage is $N \times P \times q$, where N denotes the number of power traces used and P corresponds to the number of sampling points selected per power trace, which is set to 31.

The experimental results of using different power traces for the attack are shown in **Table** 2. The critical number of power traces required to fully recover the key coefficients is the threshold, and the average Guessing Entropy (GE) is the mean of the initial Guessing Entropy for incorrectly recovered key coefficient guesses. For the shake_output_wait state, recovering 64 key coefficients requires 120000 power traces. For the finalization_SHAKE state, recovering 24 key coefficients requires 80000 power traces. For the reset state, recovering the group key coefficient requires 70000 power traces. For the idle state, recovering 64 key coefficients requires 110000 power traces. Lastly, for the shake_process and process_last_block states, recovering 32 key coefficients requires 980000 and 880000 power traces, respectively. The number of powewr traces required to recover the key coefficients is consistent with the trend shown in **Fig**. 7, with a

Table 2: The results of key recovery using different methods in different states

	method	CPA	CPA-PoI	CPA-ITR	CPA	CPA-PoI	CPA-ITR	CPA
	traces$(\times 10^4)$	6	6	6	7	7	7	/
reset	recovery ratio	5/8	6/8	8/8	8/8	8/8	8/8	/
	average GE	23/3	4/2	-	-	-	-	/
	traces$(\times 10^4)$	9	9	9	11	11	11	/
idle	recovery ratio	29/64	45/64	56/64	64/64	64/64	64/64	/
	average GE	226/3	27/2	7	-	-	-	/
	traces$(\times 10^4)$	7	7	7	8	8	8	/
finalization_SHAKE	recovery ratio	20/24	22/24	23/24	24/24	24/24	24/24	/
	average GE	87/4	13/2	4	-	-	-	/
	traces$(\times 10^4)$	9	9	9	10	10	10	12
shake_output_wait	recovery ratio	49/64	63/64	64/64	61/64	64/64	64/64	64/64
	average GE	7/3	4	-	4/2	-	-	-
	traces$(\times 10^4)$	80	80	80	83	83	83	88
process_last_block	recovery ratio	22/32	26/32	26/32	22/32	32/32	32/32	32/32
	average GE	10/2	2	2	6/2	-	-	-
	traces$(\times 10^4)$	80	80	80	87	87	87	98
shake_process	recovery ratio	21/32	29/32	32/32	28/32	32/32	32/32	32/32
	average GE	17/3	2	-	11/2	-	-	-

[1] recovery ratio: For example, $\frac{a}{b}$ denotes attacking key coefficients of b and successfully recovering a.

[2] GE denotes the Guessing Entropy, which refers to the sequence number of the correct key in the order of correlation coefficients among all key guesses.

[3] average GE: For example, in the context of $\frac{a}{b}$, where b denotes the number of initial recovery errors in the key coefficients, the sum of their GE is a.

[3] /: Indicates that the number of target key coefficients has been fully recovered.

[4] -: This indicates that the guessed entropy for all key coefficients is 1.

drastic increase in the number of power traces during the shake_process and process_last_block states, indicating a higher level of algorithmic noise during these states.

4.2 Results of the CPA-PoI Method

Based on the CPA method, the CPA-PoI method was adopted to more accurately locate the PoIs. When selecting the PoIs, we used the Hamming distance parameter $\hat{c}$ and selected 3 points. The calculation complexity in this case is $N \times P \times q$, where P is 3. Compared to the CPA method, the CPA-PoI method has a reduced calculation complexity.

According to the results in **Table** 3, compared to the CPA method, the CPA-PoI method reduces the number of power traces required to fully recover the target key coefficients by [0, 16.67%]. Even when the number of power traces is not reduced, the average GE of the CPA-PoI method is generally lower than that of the CPA method, which indicates that the effect of the CPA-PoI method can be observed by further refining the number of power traces used in the attack.

In cases where the CPA method has not fully recovered the target key coefficients coefficients, when attacking with the same number of power traces, the CPA-PoI method significantly increases the number of recovered key coefficients, with an improvement range between [10%, 55.17%]. This indicates that, with the same number of power traces, the CPA-PoI method can recover more key coefficients and achieves better results compared to the CPA method.

Table 3: Comparison of results from attacks using different methods in different states

comparison	traces used by CPA		number of key coefficients recovered by CPA		traces used by CPA-PoI	number of key coefficients recovered by CPA-ITR
method	CPA-PoI	CPA-ITR	CPA-PoI	CPA-ITR	CPA-ITR	CPA-ITR
reset	0	14.28%	20%	60%	14.28%	33.33%
idle	0	0	55.17%	93.10%	0	24.44%
finalization_SHAKE	0	0	10%	15%	0	4.54%
shake_output_wait	16.67%	25%	28.57%	30.61%	10%	1.58%
process_last_block	5.68%	5.68%	45.45%	45.45%	0	0
shake_process	11.22%	18.36%	38.09%	52.38%	8.05%	10.34%

4.3 Results of the CPA-ITR Method

Based on the CPA method, we employed the CPA-ITR method to effectively leverage parallelization for information leakage. By comparing the experimental results with the CPA and CPA-PoI methods, we derived **Table** 3.

From **Table** 3, it can be seen that compared to the CPA method, the CPA-ITR method reduces the number of power traces required to fully recover the target key coefficients by [0, 25%], and compared to the CPA-PoI method, it reduces the number by [0, 14.28%]. Additionally, the CPA-ITR method significantly decreases the average GE, which is close to that of the CPA-PoI method. When attacking with the same number of power traces, the CPA-ITR method improves the number of recovered key coefficients compared to the CPA method by [15%, 93.10%]. In comparison to the CPA-PoI method, the improvement range is [0, 33.33%]. Overall, the CPA-ITR method demonstrates significant improvement compared to the CPA method and offers certain advancements over the CPA-PoI method as well.

It is important to note that in the CPA-ITR attack, if the first attacked key coefficient is incorrectly recovered, it may cause interference in the attacks on the other three key coefficients in parallel. However, during our experiments, we observed that the recovery of the first coefficient was generally easier to achieve in our implementation.

5 Conclusion

The paper presents a practical attack on an FPGA implementation of Dilithium, This is the first work to attack a FPGA implementation of Dilithium using power leakages. We take advantage of the parallelism on FPGAs and propose CPA-PoI and CPA-ITR. The experimental results show that the proposed attack methods use fewer power traces compared to the classical CPA, and can recover more key coefficients with the same number of power traces. Our work demonstrates the feasibility of side-channel attack to polynomial multiplication operations on highly parallelised hardware. Due to the large key guessing space and the impact of algorithm noise, the attacks take a long time. In future work, we aim to find better attack strategies to efficiently recover the private key with less time.

References

1. Avanzi, R., Bos, J., Ducas, L., Kiltz, E., Lepoint, T., Lyubashevsky, V., Schanck, J., Schwabe, P., Seiler, G., Stehlé, D.: Crystals-kyber (version 2.0)-algorithm specifications and supporting documentation (april 1, 2019). Submission to the NIST post-quantum project (2019)
2. Bai, S., Ducas, L., Kiltz, E., Lepoint, T., Lyubashevsky, V., Schwabe, P., Seiler, G., Stehlé, D.: Crystals-dilithium: Algorithm specifications and supporting documentation (version 3.1). NIST Post-Quantum Cryptography Standardization Round 3 (2021)
3. Beckwith, L., Nguyen, D.T., Gaj, K.: High-performance hardware implementation of crystals-dilithium. In: International Conference on Field-Programmable Technology, (IC)FPT 2021, Auckland, New Zealand, December 6-10, 2021. pp. 1–10. IEEE (2021). https://doi.org/10.1109/ICFPT52863.2021.9609917
4. Bernstein, D.J., Hopwood, D., Hülsing, A., Lange, T., Niederhagen, R., Papachristodoulou, L., Schneider, M., Schwabe, P., Wilcox-O'Hearn, Z.: SPHINCS: practical stateless hash-based signatures. In: Oswald, E., Fischlin, M. (eds.) Advances in Cryptology - EUROCRYPT 2015 - 34th Annual International Conference on the Theory and Applications of Cryptographic Techniques, Sofia, Bulgaria, April

26-30, 2015, Proceedings, Part I. Lecture Notes in Computer Science, vol. 9056, pp. 368–397. Springer (2015). https://doi.org/10.1007/978-3-662-46800-5_15

5. Berzati, A., Viera, A.C., Chartouni, M., Madec, S., Vergnaud, D., Vigilant, D.: A practical template attack on crystals-dilithium. IACR Cryptol. ePrint Arch. p. 50 (2023), https://eprint.iacr.org/2023/050
6. Chen, Z., Karabulut, E., Aysu, A., Ma, Y., Jing, J.: An efficient non-profiled side-channel attack on the crystals-dilithium post-quantum signature. In: 39th IEEE International Conference on Computer Design, ICCD 2021, Storrs, CT, USA, October24-27, 2021. pp. 583–590. IEEE (2021). https://doi.org/10.1109/ICCD53106.2021.00094,
7. Ducas, L., Kiltz, E., Lepoint, T., Lyubashevsky, V., Schwabe, P., Seiler, G., Stehlé, D.: Crystals-dilithium: Algorithm specifications and supporting documentation. Round-2 submission to the NIST PQC project 35 (2019)
8. Ducas, L., Lepoint, T., Lyubashevsky, V., Schwabe, P., Seiler, G., Stehlé, D.: CRYSTALS - dilithium: Digital signatures from module lattices. IACR Cryptology ePrint Archive 2017, 633 (2017), http://eprint.iacr.org/2017/633
9. Ducas, L., Lepoint, T., Lyubashevsky, V., Schwabe, P., Seiler, G., Stehlé, D.: Crystals–dilithium: Digital signatures from module lattices. Submission to the NIST's post-quantum cryptography standardization process (2018)
10. Fouque, P.A., Hoffstein, J., Kirchner, P., Lyubashevsky, V., Pornin, T., Prest, T., Ricosset, T., Seiler, G., Whyte, W., Zhang, Z., et al.: Falcon: Fast-fourier lattice-based compact signatures over ntru. Submission to the NIST's post-quantum cryptography standardization process 36(5), 1–75 (2018)
11. Han, J., Lee, T., Kwon, J., Lee, J., Kim, I., Cho, J., Han, D., Sim, B.: Single-trace attack on NIST round 3 candidate dilithium using machine learning-based profiling. IEEE Access 9, 166283–166292 (2021). https://doi.org/10.1109/ACCESS.2021.313-5600
12. Moody, D.: Post-quantum cryptography standardization: Announcement and outline of nist's call for submissions. In: International Conference on Post-Quantum Cryptography-PQCrypto (2016)
13. Primas, R., Pessl, P., Mangard, S.: Single-trace side-channel attacks on masked lattice-based encryption. In: Fischer, W., Homma, N. (eds.) Cryptographic Hardware and Embedded Systems - CHES 2017 - 19th International Conference, Taipei, Taiwan, September 25-28, 2017, Proceedings. Lecture Notes in Computer Science, vol. 10529, pp. 513–533. Springer (2017). https://doi.org/10.1007/978-3-319-66787-4_25
14. Qiao, Z., Liu, Y., Zhou, Y., Ming, J., Jin, C., Li, H.: Practical public template attack attacks on crystals-dilithium with randomness leakages. IEEE Trans. Inf. Forensics Secur. 18, 1–14 (2023). https://doi.org/10.1109/TIFS.2022.3215913
15. Ravi, P., Jhanwar, M.P., Howe, J., Chattopadhyay, A., Bhasin, S.: Side-channel assisted existential forgery attack on dilithium - A NIST PQC candidate. IACR Cryptol. ePrint Arch. p. 821 (2018), https://eprint.iacr.org/2018/821
16. Ravi, P., Jhanwar, M.P., Howe, J., Chattopadhyay, A., Bhasin, S.: Exploiting determinism in lattice-based signatures - practical fault attacks on pqm4 implementations of NIST candidates. IACR Cryptol. ePrint Arch. p. 769 (2019), https://eprint.iacr.org/2019/769
17. Shor, P.W.: Algorithms for quantum computation discrete logarithms and factoring. In: 35th Annual Symposium on Foundations of Computer Science, Santa Fe, New Mexico, USA, 20-22 November 1994. pp. 124–134. IEEE Computer Society (1994). https://doi.org/10.1109SFCS.1994.365700

18. Steffen, H.M., Land, G., Kogelheide, L.J., Güneysu, T.: Breaking and protecting the crystal: Side-channel analysis of dilithium in hardware. IACR Cryptol. ePrint Arch. p. 1410 (2022), https://eprint.iacr.org/2022/1410